Climate Dynamics (1999) 15:619–629

W. T. Hyde · T. J. Crowley · L. Tarasov
W. R. Peltier

The Pangean ice age: studies with a coupled climate-ice sheet model

Received: 30 June 1998 / Accepted: 5 January 1999

Abstract Application of an ice sheet model developed for the Pleistocene to the extensive Carboniferous glaciation on Gondwana yields an ice sheet which has several features consistent with observations. While complete deglaciation is not achieved without CO_2 changes, the Milankovich-induced fluctuations in ice sheet volume are comparable to Pleistocene glacial/interglacial signals. This result is shown to hold for a large fraction of physically reasonable parameter space. The model also exhibits multiple equilibria and sharp bifurcations, as infinitesimal changes in the solar constant or precipitation can lead to a qualitatively different climate. The success of the model in predicting ice location in an environment quite different from the Pleistocene provides additional support for the robustness of the basic model physics and suggests that the model can be applied with some confidence to other pre-Pleistocene glaciations.

1 Introduction

There have been four major phases of glaciation in the last billion years (Crowell 1978; Crowley and North 1991), the late Precambrian (600–800 Ma), Late Ordovician (440 Ma), Permo-Carboniferous (275–330 Ma), and late Cenozoic (0–40 Ma). Although substantial efforts have been expended on modeling the most recent phase of Pleistocene glaciations (Crowley and North 1991), and progress has been made on identifying critical boundary conditions for inception of pre-Pleistocene glaciers (Crowley and Baum 1992, 1993, 1995; Berner 1994), there has been limited application of Pleistocene ice sheet models to the earlier glaciations in Earth history. A notable exception involves ice sheet model sensitivity studies relevant to the initiation and expansion of the Antarctic ice sheets (Huybrechts 1994). Such applications are valuable for several reasons: (1) they provide more insight into pre-Pleistocene climates; (2) they afford an opportunity for testing the robustness of the model physics; and (3) they are a critical step in the development of a comprehensive theory for glaciation in Earth history.

In this work we bring together the above two strands of research and apply a Pleistocene ice sheet model to the Permo-Carboniferous glaciation. This time period was characterized by extensive glaciation on the supercontinent of Pangea as shown in Fig. 1 (Parrish et al. 1986; Frakes et al. 1992; Ziegler et al. 1997). Prior climate modeling work suggests that the seasonal cycle on Pangea (Crowley et al. 1989; 1991; Kutzbach and Gallimore, 1989) is large enough that the climatic regime on this supercontinent was qualitatively different from that of the Pleistocene. We employ an ice sheet model (Tarasov and Peltier 1997b) that has successfully simulated the timing, location, and ice volume changes of the last glacial cycle (last 122 000 y).

W. T. Hyde (✉) · T. J. Crowley
Department of Oceanography. Texas A&M University,
College Station. TX 77843-3146, USA
E-mail: hyde@rossby.tamu.edu

L. Tarasov
Department of Geography, University of Georgia,
Athens, GA 30602-2502, USA

W. R. Peltier
Department of Physics, University of Toronto,
Toronto, Ontario, Canada M5S 1A7

2 Model description

The model of Tarasov and Peltier consists of four major components, which are modeled as follows:

1. Ice height is predicted by a two dimensional vertically integrated ice sheet model based on the Nye formulation (Nye 1959), in which both internal deformation and basal sliding are accounted for by a strong shearing flow near the bedrock, and the shallow ice approximation is used.
2. The ice sheet is coupled to a local damped-return to equilibrium bedrock model with a relaxation time of 5000 y. While the actual

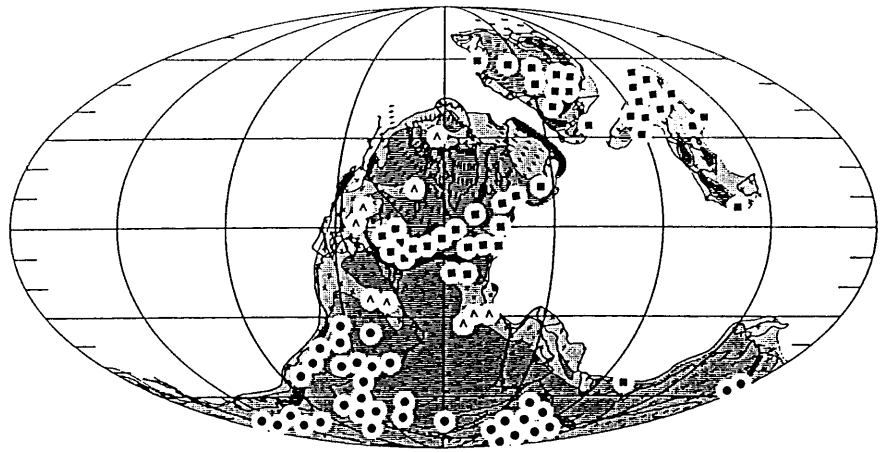

Fig. 1 Evidence for extensive Carboniferous glaciation on Gondwana. Figure illustrates Westphalian ($\approx$ 306 Ma) paleogeography and distribution of climatically controlled sediments after Parrish et al. (1986). Key: *circles*, tillites (glacial deposits); *squares*, coals (indicating high moisture), *inverted* "*v*", evaporates (indicating low moisture); *dark shading*, highland; *medium shading*, lowland; *light shading*, continental shelf

physics of the bedrock response is more complicated, this simple model provides a reasonable approximation to the detailed viscoelastic model (Tarasov and Peltier 1997a; Peltier 1996).

3. The ice model is driven by a mass balance model modified from those of Reeh (1990) and Huybrechts and T'Siobbel (1995). This itself has two distinct components, precipitation and ablation. Ablation is determined through a heating degree day formulation. Given the monthly mean temperature, the number of heating degree days is computed by a normal statistical model with a standard deviation in daily temperatures of 5.5 °C. The melting rate is set proportional to the yearly total of heating degree days, with snow and ice melting at different rates, snow being melted first, and excess energy used to melt ice. Sixty percent of the snowmelt is assumed to refreeze and snow which survives the year is assumed to become ice. The precipitation model requires as input a base precipitation field, which for the Pleistocene simulations of Tarasov and Peltier (1997b) was taken from present day monthly climatology. This base field is then modified for changes in temperature (through an exponential approximation to the Clausius-Clapeyron equation) and elevation (precipitation is reduced through an "elevation desert" effect when the ice sheet surface is above 2 km in height). The fraction of precipitation which falls as snow is also determined by a statistical model based on mean monthly temperatures, as in Reeh (1990).
4. The required temperature fields are computed by a modified version of the two dimensional nonlinear energy balance model (EBM) originally presented in North et al. (1983) and generalized in Hyde et al. (1990). The EBM is a spectral model, the temperature fields being solved to eleventh order in a spherical harmonic expansion and to second order (annual mean, annual cycle, and semi-annual cycle) in time. The model resolves the seasonal cycle of temperatures as a function of geography with seasonal snow and sea ice fields being computed by a critical temperature rule. As discussed in Hyde et al. (1990), the EBM best reproduces the current climate if land surfaces are regarded as snow covered when the average monthly temperature is below $-2\,^{\circ}$C, and the critical temperature for sea ice is taken to be $-4\,^{\circ}$C, the two degree gap representing the lower freezing point of seawater. Continental areas are represented as having a very low heat capacity (essentially that of the atmospheric column) while the oceans are represented by a mixed layer of about 75 m thickness with a much higher heat capacity. As a result the seasonal cycle over the ocean is small, while that far inland is large. Given that a small seasonal cycle is favorable for the growth of ice sheets, the degree of continentality and oceanic influence will be a key factor in determining the locations of ice sheet nucleation. Numerous intercomparisons indicate that this model has a sensitivity comparable to that of more complex general circulation models (Crowley et al. 1991).

   The EBM can be applied in one of two distinct models. If we wish to simulate a climate not too radially different from one we know well (e.g., the current climate) the model can be run in perturbative mode. In this case the mean monthly temperature consists of the base (e.g., contemporary) value, plus a perturbation computed by the EBM due to orbital, albedo, and topographic change. This approach has the advantage that features not included in the EBM (e.g., the effect of the Tibetan Plateau) are retained in the temperature field. If we do not have a base temperature field, the EBM can be run in forward mode, in which temperature is computed directly, as in Hyde et al. (1990). For our Carboniferous experiments we employ the EBM directly rather than in perturbative mode.
5. No ice shelf dynamics are included in the model, ice flowing into the ocean is removed by an artificially large ablation rate which simulates calving. Although the ice model employed in this work contains several simplifying assumptions, a fully three-dimensional thermomechanical version of the model yields no significant difference in predicted Pleistocene ice volume, though a marked improvement in the topographic structure of the predicted Pleistocene ice sheets does result (Tarasov and Peltier 1999).

The ice and bedrock equations were solved on a 0.5×0.5 degree grid, with a model domain from 85 °S to 35 °S (the three million year run discussed in Sect. 3 was run on a slightly smaller domain, extending south to 80° – owing to the nature of the differential equation solver the simulation time increases rapidly the closer the ice is allowed to approach the pole). No ice was allowed to flow through the southern boundary, nor was ice allowed to accumulate in the Northern Hemisphere (though the EBM does predict snow and sea ice there, and the albedo effect of these fields on temperature is included). We will defer discussion of a possible Siberian ice sheet to a later paper.

3 Carboniferous boundary conditions

For the Carboniferous (Westphalian) simulations (306 Ma) model inputs include paleogeography, Milankovitch forcing, CO_2 levels, topography, precipitation, and the solar constant. Paleogeography and topography are taken from Scotese (1986), while the average height of the land surface where no topography is specified is taken to be zero. In Sect. 5 we will test the sensitivity of the model to these paleogeographic boundary conditions.

In order to minimize the number of adjustable parameters in the model, our base precipitation was initially taken to be the average of current Northern Hemisphere land values and also constant in space and time (though this base value is modified by temperature and elevation changes as described above). While this choice is somewhat arbitrary, it allows easier comparison with the Pleistocene results of Tarasov and Peltier (1997b) and is qualitatively resonable in that Eurasia is the closest analog to Gondwana of today's land

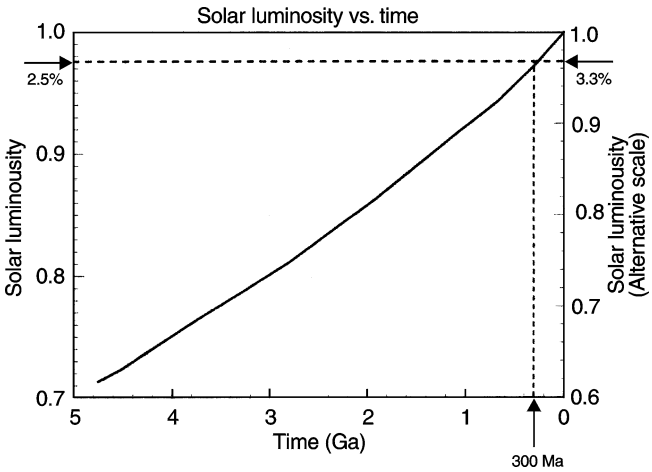

Fig. 2 Evolution of solar luminosity versus time as computed in Endal and Sofia (1981) and scaled by Crowley et al. (1991). Two different scales are used, representing different estimates of the initial composition of the Sun's core, and hence of initial luminosity

masses. In Sect. 5 we will present sensitivity experiments with a number of somewhat more realistic input precipitation fields.

Geochemical models (Berner 1994), which have been semi-quantitatively validated against proxy CO_2 data (Berner 1997), suggest that CO_2 levels for the Carboniferous were approximately the same as at present. We therefore used contemporary CO_2 levels (exept where otherwise specified) and did not change CO_2 during glacial cycles as is done in Tarasov and Peltier (1997b).

Though the periods of variation in longitude of perihelion and obliquity were slightly different at 300 Ma, the differences are less than 10% (Berger et al. 1989). We have therefore used the Milankovitch forcing appropriate to the next four million years in our simulations (Berger 1978).

A key input for model simulations is solar luminosity. Solar models suggest that the insolation at this time was $\approx$2.5–3.3% below contemporary values (Endal and Sofia 1981; Crowley et al. 1991) (Fig. 2). EBM studies and general circulation model (GCM) work (Crowley et al. 1991; Crowley and Baum 1994) indicate that the large seasonal cycle on Gondwana renders summer temperatures too high for the survival of ice year round without some decrease in solar constant.

4 Baseline experiment

We first discuss a 3.2 million year long baseline experiment with boundary conditions as specified above, and a solar constant taken to be 3% below the current value. In this case, the model predicted ice sheet nucleates on the West Antarctic coast, eventually growing extremely large ($\approx 150 \times 10^6 km^3$) and covering the bulk of Gondwana (Fig. 3). For comparison, model predicted ice volume (North America and Eurasia) at the last glacial maximum is about 35×10^6 km^3, in reasonable agreement with observations (Peltier 1994). At maximum the ice extends to 45 °S and is consistent with some reconstructions of Carboniferous glaciation (Parrish et al. 1986; Powell and Veevers 1987; Ziegler et al. 1997; Scotese and Golonka, 1992; Eyles 1993). In particular, the ice sheet border in northern Africa (Fig. 3) agrees well with a recent estimate of the northern limit of glaciation (Wopfner and Casshyap 1997). The most significant model-data discrepancies involve possible overestimation of ice extent in the east African sector and failure to simulate an extension of ice as far north as 30 °S along western South America. The former response could reflect a uniform precipitation field; one would expect some reduction of ice in this area due to the normal pattern of decreased moisture in continental interiors. On the other hand, some sources (e.g. Visser 1997) place ice in the Congo basin, though at present the dating of these deposits is not sufficiently precise for us to claim that they are contemporaneous with our modeled ice sheets.

With respect to South America the difficulty is that there is a plethora of possible explanations for the model's failure. For example, we could possibly induce the model to glaciate this area by increasing local precipitation or topography, incorporating an epicontinental sea over part of South Africa, or mimicking a cold eastern boundary current off the coast. All of these changes are plausible, given the degree to which the boundary conditions are known. Additionally, the glacial deposits in this area might have resulted from mountain or piedmont glaciers, rather than a large ice sheet. Better input data and a higher resolution climate model are required before this question can be rigorously addressed. Nevertheless in the next section we will attempt to evaluate several of the above possibilities.

Our modeled ice sheets are almost always single-domed, though Carboniferous reconstructions (e.g., Eyles 1993) are multi-domed and separate. While this may again be due to an excessively simple topography or precipitation pattern, there is reason to believe that this problem will be better addressed through a fully coupled thermomechanical model (Tarasov and Peltier 1999). It is also possible that the incompleteness of the geologic record could lead to a misinterpretation of Carboniferous ice sheet dimensions.

While there is no deglaciation in the baseline run, the ice sheet fluctuates substantially under Milankovitch forcing (Fig. 4). The warm "precessional summers" cause a considerable retreat of ice in the more continental locations (Fig. 3), while areas which are far south and/or have a marine-influenced climate are relatively unaffected. This response is qualitatively different than GCM "hot summer orbit" studies (Crowley and Baum 1994; Valdes and Crowley 1998) for the Carboniferous with no ice sheet; the latter studies simulate a complete removal of snow cover on the very large Gondwanan land mass. The fluctuations evident in Figs. 3 and 4 involve the rapid melting of as much as fifty million cubic kilometers of ice, with consequent eustatic sea level change on the order of a hundred meters, as large as the Pleistocene glacial/interglacial changes which resulted in a near-complete removal of ice from North America and Eurasia. The estimated sea

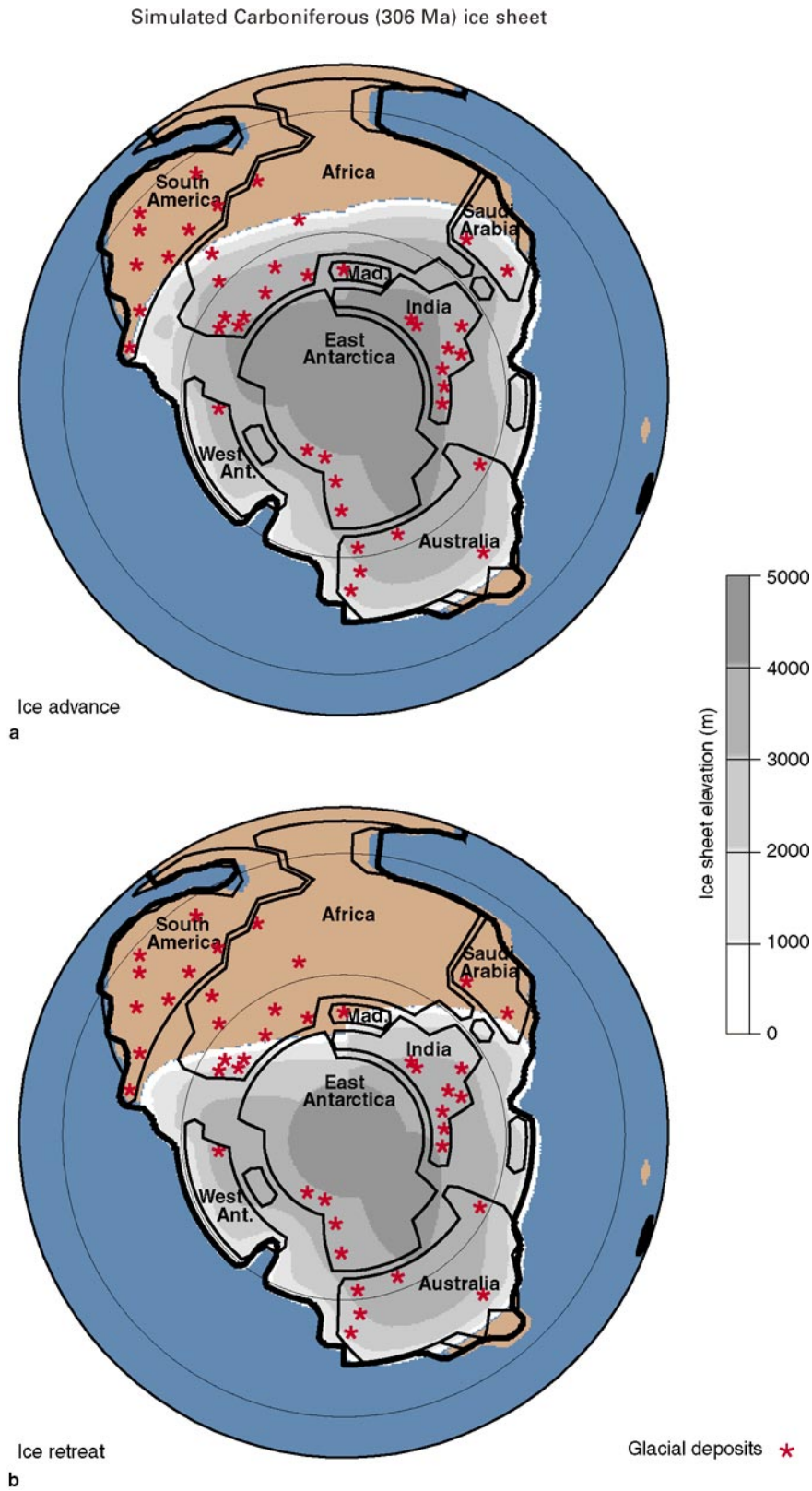

Fig. 3a,b Ice sheet thickness at a local maximum (224 ky into the baseline run) and minimum (at 237 ky), see Fig. 4. *Asterisks* indicate the location of glacial deposits (from Crowley and Baum 1992 and after Parrish et al. 1986; Powell and Veevers 1987; Eyles 1993; Visser 1997). For computational reasons the model domain does not extend south of 80 degrees. Though ice is presumed in this figure to exist south of this latitude it is not included in our volume calculations

level changes are comparable to those observed in North American cyclothem sequences (Crowley and Baum 1992; Klein and Willard 1989; Heckel 1994; Rasbury et al. 1998), which have long been linked to Gondwanan ice volume changes (Wanless and Shepard 1936).

The model predicts a long-term anticorrelation between ice volume and orbital eccentricity. This is

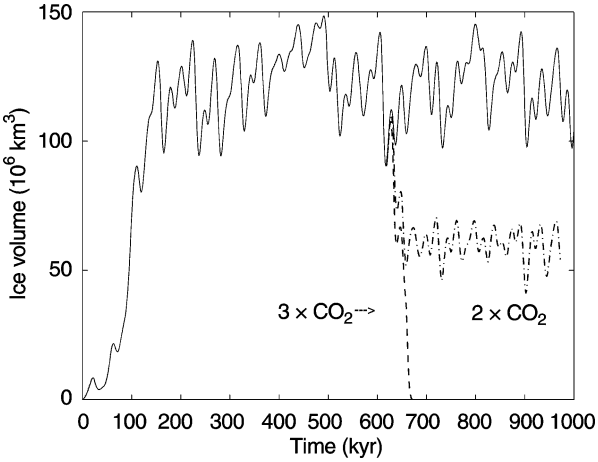

Fig. 4 Eight hundred thousand years of a baseline Carboniferous run with a solar constant 3% below present. Also shown are the results of two further sensitivity experiments involving increases in CO_2 from current to 3X, and current to 2X present values with concentration increasing linearly for 50 000 y beginning at model year 617 000

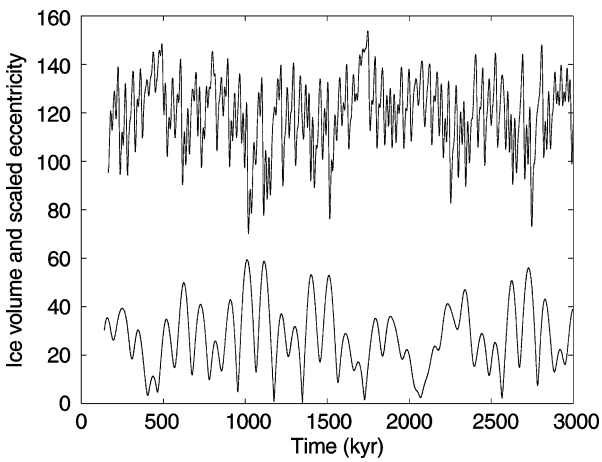

Fig. 5 Three million years of the baseline run ice volume in millions of cubic kilometers (*upper curve*) compared with orbital eccentricity scaled by one thousand

clearly demonstrated in Fig. 5 where we show three million years of the baseline run (the short growth phase is omitted) compared with orbital eccentricity. The same result was obtained in Hyde and Peltier (1987), though for a simpler ice model and shorter time series. This result is consistent with the Köppen-Milankovitch hypothesis (Milankovitch 1930), i.e., in times of high eccentricity "precessional summers" (those periods for which perihelion occurs in summer) are particularly warm, resulting in melting.

Strong eccentricity forcing is also evident in a spectral analysis of the ice volume time series (Fig. 6). For comparison we have plotted on the same graph a spectral analysis of the five million year detrended Plio–Pleistocene oxygen isotope record (Clemens and

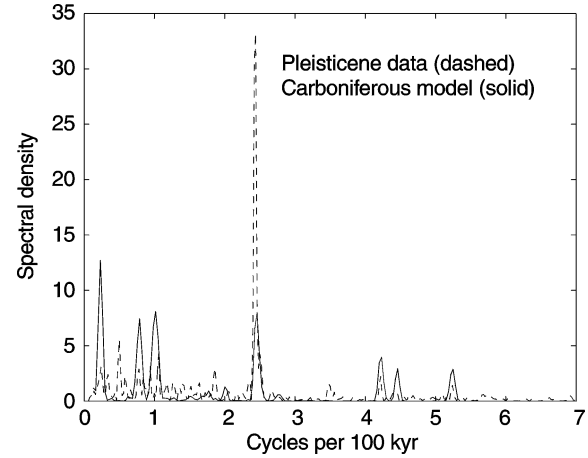

Fig. 6 Periodogram of three million years of model output (*solid*) and five million years of isotope data (*dashed*, from Clemens and Tiedemann 1997). Strong response is evident in model output at all Milankovitch frequencies, with significant variance at the longer frequencies (100 ka and 400 ka)

Tiedemann 1997). All of the dominant periodicities in the astronomical forcing are represented in the model output, with substantial 100 ka (thousand year) and 400 ka power despite the absence of glacial/interglacial CO_2 changes. This model response may reflect the amplification of 100 ka and 400 ka forcing by the large Pangean land mass (Crowley et al. 1992). Earlier work (Heckel 1986; Algeo and Wilkinson 1988) interpreted the cyclicity of mid-continent USA. Carboniferous sequences as consistent with 400 ka power, though a recent paper by Rasbury et al. (1998) argues that this cyclicity is actually more consistent with the shorter 100 ka eccentricity period. The latter paper does not, however deal with the question of the presence or absence of 400 ka power. Despite the highly nonlinear nature of the model, there is no significant power at sum frequencies (approximately 10 000 y periodicities); however, the ice sheet has a low-pass bias, with the amplitude of low frequency variations being enhanced relative to the forcing.

5 Sensitivity experiments

We conducted a number of studies of the model's response to changes in our inputs: CO_2, the solar constant, precipitation, and topography.

Carbon dioxide

Geochemical model calculations suggest that an increase in CO_2 may have occurred in the Permian (Berner 1994). The actual timing of the postulated Permian CO_2 increase requires more precise testing. For example, it is not clear whether carbon isotope

studies (Grossman 1994) support a mid-Sakmarian ($\approx$275 Ma) carbon dioxide increase coincident with the observed end of the major phase of Permo-Carboniferous glaciation.

The baseline run was therefore perturbed, beginning 617 ky after the start of the run, with CO_2 increasing linearly over the next 50 000 y. For the $3 \times CO_2$ case the model rapidly deglaciates (Fig. 4) and has no difficulty maintaining an ice-free state despite later Milankovitch cooling episodes. Further studies with $2 \times CO_2$ do not produce deglaciation. Rather, the ice sheet settles into a new equilibrium about half as large as that with contemporary CO_2 levels. This result suggests that the ice sheet system has a hysteresis, as this state is not attainable by direct growth from an initially ice free condition. This hysteresis may be related to the bifurcation discussed below.

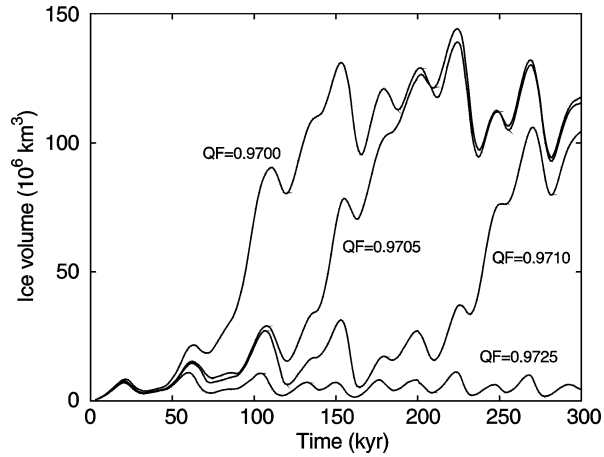

Fig. 7 Model results indicating that small variations in the solar constant (QF) can have a profound effect on ice sheet volume

Solar constant

The ice sheet model exhibits critical behavior (Fig. 7). While very small changes in the solar constant (e.g. between a constant 0.9700 of present and 0.9705) can delay the onset of full glaciation by upwards of 100 000 y, at the critical point a simulation with a solar constant of 0.9720 grows to a large ice sheet after some 400 000 y of integration, while for a solar constant of 0.9725 times present the small coastal ice sheet never expands into the interior of Gondwana. The difference in net radiative forcing between the two different ice sheet states is about one-twentieth the Pleistocene ice age CO_2 radiative perturbation and about the same as solar irradiance changes associated with the 11-y cycle. This extremely small perturbation highlights the bistable nature of the modeled ice sheet response. Note that for no value of the solar constant does the ice sheet evolve to the intermediate size seen in the doubled CO_2 experiment.

While this transition from the small to large equilibrium states (e.g. Fig. 7, for QF = 0.9710) was not found in a recent ice sheet modeling study we do not feel that this disparity is a problem. In the paper in question (Morales Maqueda et al. 1998), the continent simulated was Antarctica, which is smaller and far more maritime than Gondwana, the simulations performed were a relatively short 40 ky (it can be seen in Fig. 7 that our transitions can take far longer), and finally the ice sheet resolution in Morales Maqueda et al. (1998) was rather coarse.

Although it is beyond the scope of this work to investigate in detail the bistable response of the ice sheet model, we note that other studies (Baum and Crowley 1991; Crowley et al. 1994; Otto-Bliesner 1996) have found critical behavior in Gondwanan snow-cover in GCM and EBM simulations. However, the criticality exhibited in Fig. 7 is intrinsic to the ice sheet. For these and nearby values of the solar constant there is no equivalent jump in EBM predicted snow area.

With respect to the physical processes associated with the bifurcation, EBM studies (Crowley et al. 1987; Hyde et al. 1990; Baum and Crowley 1991) suggest that because of the moderating effect of large bodies of water on seasonal warming, coastal areas are most likely to remain cold enough in summer to allow the preservation of ice. For the Carboniferous, this is all the more plausible as the coastal ice sheet is located in one of the principal areas of elevated topography. Thus the existence of a small coastal ice sheet is consistent with previous work. On the other hand, if some favorable orbital configuration allows a very large ice sheet to form, the elevation and high albedo of the ice sheet will drastically lower the temperature, while the albedo will also greatly weaken the seasonality, so that a "precessional summer" may not be warm enough, or last long enough (given the long time constants of large ice sheets) to destroy the ice sheet. Thus it is physically reasonable that a very large ice sheet is also stable, while a moderate-sized ice sheet may not be (Raymo 1997).

This conjecture requires considerable additional analysis which we intend to address in a followup paper. Conceivably this bistable ice sheet response could provide insight into some of the rapid transitions in Plio–Pleistocene climate at around 2.6 and 0.9 Ma (Shackleton and Opdyke 1976; Shackleton et al. 1984).

Precipitation

To test the sensitivity of the model to changes in precipitation, we created several artificial base precipitation fields intended to mimic the expected dryness of the interior of Gondwana. In these fields the precipitation decreased linearly (by an amount θ mm/day per

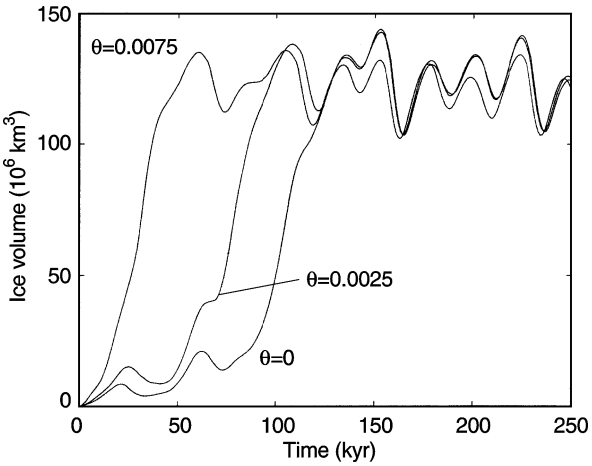

Fig. 8 The effect of redistributing precipitation on Gondwana. Precipitation decreases by θ mm/day per degree from the coast while all fields are normalized to have the same average precipitation. Thus coastal precipitation increases with θ, while interior precipitation decreases. While the ice sheet grows more rapidly for high values of θ, the final equilibrium state is insensitive to this parameter

degree) with distance south from the coast. The resulting precipitation field was normalized so that land areas between 35 and 85 °S had the same average precipitation (0.6 mm/day) as in the baseline experiment. Our values of θ were chosen such that the largest yielded six times as much precipitation (1.2 mm/day) on the coastline as in the interior (0.2 mm/day) in rough agreement with contemporary interior-coastal differences from Eurasia (Legates and Willmott 1990). Actual precipitation is more variable in space than our artificial fields, and further simulations need to be made with more realistic inputs, perhaps taken from GCM output.

The model's sensitivity to the slope of the precipitation line is similar to its sensitivity to solar constant (Fig. 8) in that the rate at which the large equilibrium state is achieved is dependent on θ, but the nature of the equilibrium is relatively insensitive to this parameter. Given that the baseline run ice sheet first nucleates on the coast, it is understandable that a higher θ, meaning higher coastal precipitation, causes a more rapid onset, while a lower θ, which puts more precipitation in the interior where it is melted off in warm continental summers, results in a more slowly growing ice sheet. As the expansion of the large ice sheet is restricted over most of its perimeter by calving into the ocean, rather than by a warm ablation zone, it is not surprising that for the large ice sheet the integrated total of precipitation is more important than the regional details of its distribution. The very sharp decline in ice sheet height at most marine boundaries indicates that there is in fact more precipitation than is needed to maintain the areal extent of the ice sheet.

CGM experiments in Kutzbach and Gallimore (1989) and Crowley and Baum (1994) indicate that the large Pengean land mass could lead to an overall lowering of precipitation 30–50% below present values. We therefore ran experiments with three quarters (0.45 mm/day) and half (0.3 mm/day) of our baseline precipitation. With θ equal to zero, forcing with either of these lower base amounts results in a small ice sheet which forms over the higher elevations in West Antarctica, though with the larger precipitation amount the ice also covers some of the lowlands extending towards East Antarctica (Fig. 9a, b). The drier climates are more sensitive to the horizontal distribution of precipitation. In Fig. 9c it is clear that a large value of θ greatly increases the size of the ice sheet with a base precipitation of 0.3 mm/day, while the effect on the ice sheet forced by an average of 0.45 mm/day is even more dramatic (Fig. 9d). Thus we see that the sensitivity of the ice volume of θ has a minimum in both very wet climates (because there is always more than enough water to form the ice sheet) and, obviously, in very dry climates but has at least one maximum in moderate moisture regimes.

For the case of uniform precipitation, variations in the base amount produce a rapid change from a regime of small ice sheets similar to those of Fig. 9a, b, and large ice sheet characteristic of Fig. 3. The transition occurs between base precipitation values of 0.585 and 0.590 mm/day. The behavior is very similar to that of Fig. 7 in that for points just above the bifurcation value some hundreds of thousands of years are required to reach the large equilibrium.

Topography

Ice sheet/climate models are also sensitive to changes in the underlying topography (Tarasov and Peltier 1997b). There are in principle two aspects to this. The existence of localized areas of high elevation can provide nucleation sites for the ice sheet due to intense localized cooling, while a higher average elevation for the land as a whole favors ice sheet growth everywhere.

We have tested the sensitivity to average continental elevation by adding uniform height fields of 50 and 100 m to the Scotese topography (Fig. 10). Again we see that the principal effect is on the rate at which ice sheets achieve equilibrium, but in this case there is a somewhat greater effect on the final large equilibrium state than in the experiments with variable precipitation or solar constant. This seems to be due to a greater northward extent of the ice sheet over Africa, where the increased elevation has a larger effect on temperature than the small solar constant differences in Fig. 7.

In another series of tests (not shown) we tested the models response to various scalings of the Scotese topography, which essentially amounts to raising or lowering the heights of mountainous areas while leaving the plains at sea level. With zero topography ice does not develop unless the solar constant is reduced to

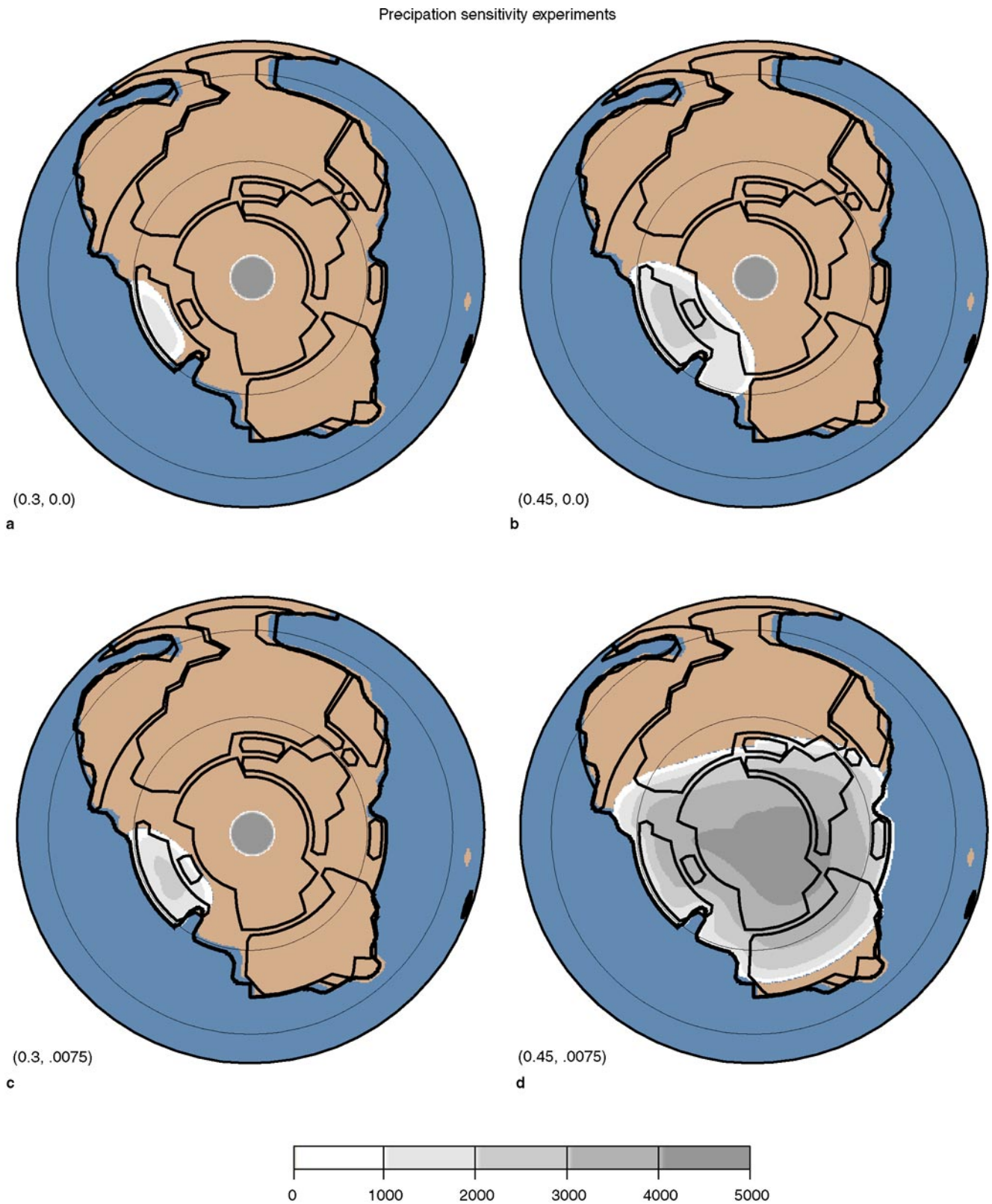

Fig. 9a–d Ice sheets in dry climates. *Bracketed numbers* refer to precipitation in mm/day, and to the decline in precipitation with distance from the coast (θ). Dry climates with uniform precipitation result in much smaller equilibrium ice sheets (**a**, **b**). These climates are far more sensitive to the distribution of precipitation and large values of θ lead to larger and even continental sized ice sheets (**c**, **d**)

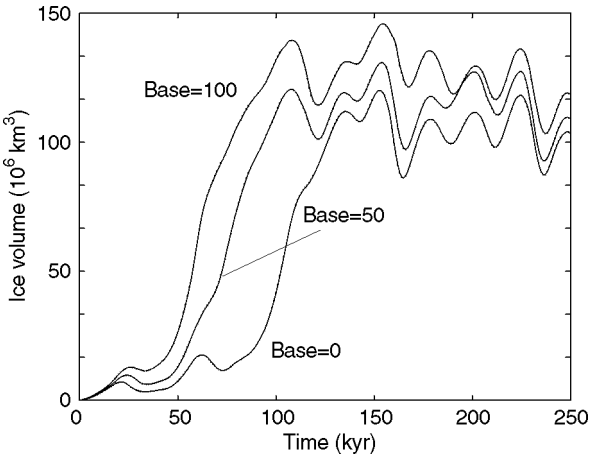

Fig. 10 Effect of uniformly adding a fixed amount (*base*) to the Scotese (1986) topography. Large values lead to cooler climates and accelerate the onset of a large ice sheet. The final equilibrium states vary mainly in the northward extent of the ice sheet over Africa

less than the 3.3% decline allowed by solar models. This is similar to the result of Tarasov and Peltier (1997b) for the Pleistocene, as in their simulations ice nucleated only on high ground in the Arctic and consistent with the work of Powell and Veevers (1987). In general we observed the same pattern as in our solar constant and precipitation experiments, doubled or tripled topography causes the ice sheet to grow more rapidly, but the equilibrium state is little affected. Although the ice sheet extends somewhat further north in the South American sector, the improvement is far too small to account by itself for our model/data discrepancy in that area.

In a final experiment (not shown) we tripled the Scotese topography and doubled precipitation over South America south of 30 °S. Naturally this resulted in somewhat greater ice cover, including a small secondary dome in South America, but three of the South American glacial sites remained ice free, and it does not seem that any reasonable combination of topography and precipitation will cause the model to extend ice into such low latitudes.

6 Discussion and conclusions

The principal result of this work has been to show that the Tarasov and Peltier ice sheet/EBM model can, with reasonable inputs and without any modification of model parameters, simulate many of the features of the Carboniferous ice age. Particular strengths of the model include prediction of sea level fluctuations consistent with observed cyclothems and the broad concordance between observations and predictions of glacial ice. It is also reassuring that the model does not predict ice during later eras of high CO_2, and indeed predicts a full deglaciation for a tripling of CO_2 levels. The model also exhibits multiple stable states which are connected with ice-albedo feedback (and elevation-temperature feedback) but in a manner different from the small ice cap instability of North (1984). This bifurcation requires further investigation.

We regard these results as strong support for the general validity of the Tarasov and Peltier model, given the very different nature of the Carboniferous and Pleistocene ice sheets. Nevertheless, deficiencies exist, e.g., the failure to predict ice over parts of South America, possible excess ice over parts of Africa, and the tendency of the model to predict one large ice sheet with one dome, rather than separate ice sheets or a multi-domed structure. In the future we hope to address these weaknesses by considering the effect of warm and cold currents and epeiric seas. It will be difficult to test the model more rigorously without a more comprehensive paleo-database. Specifically, we need to know more about the location of ice and direction of ice flow.

Additional uncertainties involve tectonic boundary conditions. Some Gondwanan reconstructions differ significantly from the one used in this work, e.g., Smith and Hallam (1970) and Scotese (1994), both of which place South America further south than the reconstruction we used. Use of the former configuration, in particular, should greatly reduce the model/data discrepancy in South America. The location and depth of inland seaways will also have an effect on ice sheet location, particularly at the onset of glaciation. The west-to-east migration of the locus of the Gondwanan ice sheet from Africa–South–America to Australia during the Permo–Carboniferous (Gonzalez-Bonorino and Eyles 1995; Lindsay 1997; Isbell et al. 1997) may reflect other landmass movements that we have not yet considered; the present simulation reflects approximately the midpoint of that long period of glaciation. GCM studies may aid in refining some model inputs, while a better understanding of the Carboniferous ocean circulation could improve regional features of the ice sheet response.

A major remaining uncertainty concerns the similar roles of continental elevation, solar constant, and CO_2 in determining Pangean ice volume. For example, though our baseline run was performed with a base height for Pangea at sea level, a qualitatively similar result could have been obtained with some combination of higher base height and higher solar constant/lower CO_2 level. Thus the available Southern Hemisphere data do not constrain these three parameters as much as we would like. However, we may be able to reduce the area of admissible parameter space in these variables by considering the presence, or otherwise, of Northern Hemisphere ice sheets. Preliminary experiments show that the parameters of the baseline run result in an ice sheet on Siberia which appears to be larger than observations allow. Thus it appears that an

optimal fit to the evidence requires some combination of higher CO_2 or solar constant, and a higher freeboard for Pangea, in agreement with observations (J. Parrish personal communication).

Despite this list of qualifications it must be borne in mind that there is considerably more agreement than disagreement between model and data, and that our results have been obtained without any retuning of the model, and with a minimum number of adjustments to model boundary conditions. In conclusion, we find that an ice sheet model developed for the Pleistocene predicts Gondwanan ice in locations approximately consistent with observations and that modest charges (from a geological viewpoint) in CO_2 can cause the melting of a very large ice sheet. As this result was achieved without tuning any of the model parameters, the basic accuracy of the model physics and formulation is therefore supported. Our results also suggest that the model can be usefully applied to other pre-Pleistocene glacial periods, e.g., the Oligocene expansion in Antarctica (Zachos et al. 1992; Huybrechts 1994), and Ordovician glaciation (Hambrey 1985; Crowley and Baum 1995) of Gondwana, and the very extensive late Precambrian glaciation (Hambrey and Harland 1985). Such efforts should open the door more widely to testing and development of a comprehensive theory for glaciation in Earth history.

Acknowledgements This research was supported by NSF grants ATM-9529109 (TJC) and OPP-9615011 (WTH). We thank S. K. Baum, S. C. Clemens, M. T. Gibbs, J. T. Parrish, N. Eyles and E. L. Grossman and advice and input.

References

Algeo TJ, Wilkinson BH (1988) Periodicity of mesoscale Phanerozoic sedimentary cycles and the role of Milankovitch orbital modulation. J Geol 96 : 313–322

Baum SK, Crowley TJ (1991) Seasonal snowline instability in a climate model with realistic geography: application to Carboniferous ($\approx$300 Ma) glaciation. Geophys Res Lett 18 : 1719–1722

Berger A (1978) Long-term variations of daily insolation and Quaternary climate changes. J Atmos Sci 35 : 2362–2367

Berger A, Loutre MF, Dehant V (1989) Influence of the changing lunar orbit on the astronomical frequencies of pre-Quaternary isolation patterns. Paleooceanography 4 : 555–564

Berner RA (1994) GEOCARB II: a revised model of atomospheric CO_2 over Phanerozoic time. Am J Sci 294 : 56–91

Berner RA (1997) The rise of plants and their effect on weathering and atmospheric CO_2. Science 276 : 544–546

Clemens SC, Tiedemann R (1997) Eccentricity forcing of Pliocene–early Pleistocene climate revealed in a marine oxygen-isotope record. Nature 385 : 801–804

Crowell JC (1978) Gondwanan glaciation, cyclothems, continental positioning, and climate change. Am J Sci 278: 1345–1372

Crowley TJ, North GR (1991) Paleoclimatology. Oxford University Press, Oxford, UK

Crowley TJ, Baum SK (1992) Modeling late Paleozoic glaciation. Geology 20 : 507–510

Crowley TJ, Baum SK (1993) Effect of decreased solar luminosity on Late Precambrian ice extent. J Geophys Res 98 : 16723–16732

Crowley TJ, Baum SK (1994) General circulation model study of late Carboniferous interglacial climates. Paleoclimates 1 : 3–21

Crowley TJ, Baum SK (1995) Reconciling late Ordovician (440 Ma) glaciation with very high (14 $\times$) CO_2 levels. J Geophys Res 100 : 1093–1101

Crowley TJ, Mengel JG, Short DA (1987) Gondwanaland's seasonal cycle. Nature 329 : 803–807

Crowley TJ, Short DA, Hyde WT (1989) Seasonal cycle variations on the supercontinent of Pangaea. Geology 17 : 457–460

Crowley TJ, Baum SK, Hyde WT (1991) Climate model comparisons of Gondwana and Laurentide glaciations. J Geophys Res D5 : 9217–9226

Crowley TJ, Kim K-Y, Mengel JG, Short DA (1992) Modeling 100 000-year climate fluctuations in pre-Pleistocene time series. Science 255 : 705–707

Crowley TJ, Yip K-JJ, Baum SK (1994) Snowline instability in a general circulation model: application to Carboniferous glaciation. Clim Dyn 10 : 363–376

Endal AS, Sofia S (1981) Rotation in solar-type stars: I Evolutionary models for the spin-down of the sun. Astrophys J 243 : 625–640

Eyles N (1993) Earth's glacial record and its tectonic setting. Earth-Sci Rev 35 : 1–248

Frakes LA, Francis JE, Syktus JI (1992) Climate modes of the Phanerozoic. Cambridge University Press, Cambridge, UK

Gonzalez-Bonorino G, Eyles N (1995) Inverse relation between ice extent and the late Paleozoic glacial record of Gondwana. Geology 23 : 1015–1018

Grossman EL, (1994) The carbon and oxygen isotope record during the evolution of Pangaea: Carboniferous to Triassic. In: Klein GD (ed) Pangaea: paleoclimates, tectonics, and sedimentation during accretion, zenith and breakup of a supercontinent. The Geological Society of America Special Paper 288 : 207–228

Hambrey HA (1985) The late Ordovician-early Silurian glacial period. Paleogr Paleoclimatol Paleoecol 51 : 273–289

Hambrey HA, Harland WB (1985) The late Proterozoic glacial era. Paleog Paleoclimatol Paleoecol 51 : 255–272

Heckel PH (1986) Sea-level curve for Pennsylvanian eustatic marine transgressive-regressive depositional cycles along midcontinent outcrop belt, North America. Geology 14 : 330–334

Heckel PH (1994) Evaluation of evidence for glacio-eustatic control of marine Pennsylvanian cyclothems in North America and consideration of possible tectonic effects. In: Tectonic and eustatic controls on sedimentary cycles, SEPM concepts in sedimentology and paleontology, 4 : 65–87

Huybrechts P (1994) Formation and disintigration of the Antarctic ice sheet. Ann Glaciol 20 : 336–340

Huybrechts P, T'Siobbel S (1995) Thermomechanical modelling of Northern Hemisphere ice sheets with a two-level mass-balance parametrization. Ann Glaciol 21 : 111–116

Hyde WT, Peltier WR (1987) Sensitivity experiments with a model of the ice age cycle: the response to Milankovitch forcing. J Atmos Sci 44 : 1351–1374

Hyde WT, Kim K-Y, Crowley TJ, North GR (1990) On the relationship between polar continentality and climate: studies with a nonlinear energy balance model. J Geophys Res D11 : 18653–18668

Isbell JL, Seegers GM, Gelhar GA (1997) Upper Paleozoic glacial and postglacial deposits, Central Transantarctic Mountains, Antarctica. In: Martin PI (ed) Late glacial and postglacial environmental changes: Quaternary, Carboniferous–Permian, and Proterozoic. Oxford University Press, Oxford, pp 230–242

Klein G de V, Willard DA (1989) Origin of the coal-bearing Pennsylvanian cyclothems of North America. Geology 17 : 152–155

Kutzbach JE, Gallimore RG (1989) Pangaean climates: megamonsoons of the megacontinent. J Geophys Res 94 : 3341–3357

Legates DR, Willmott CJ (1990) Mean seasonal and spatial variability in gauge-corrected global precipitation. Int J Clim 10 : 111–127

Lindsay JF (1997) Permian postglacial environments of the Australian plate. In: Martini PI (ed) Late glacial and postglacial environmental changes: Quaternary, Carboniferous–Permian, and Proterozoic, Oxford University Press, pp 213–229

Milankovitch MM (1930) Mathematische Klimatlehre und astronomishe Theorie der Klimaschwankungen. In: Köppen I, Geiger R (eds) Handbuch der Klimatologie. Gebrüder Borntraeger, Berlin
Morales Maqueda MA, Willmott AJ, Bamber JL, Darby MS (1998) An investigation of the small ice cap instability in the Southern Hemisphere with a coupled atmosphere-sea ice-ocean-terrestrial ice model. Clim Dyn 14 : 329–352
North GR (1984) The small ice cap instability in diffusive climate models. J Atmos Sci 32 : 1301–1307
North GR, Mengel JG, Short DA (1983) Simple energy balance model resolving the seasons and continents: application to the astronomical theory of the ice age. J Geophys Res 99 : 6576–6586
Nye JF (1959) The motion of ice sheets and glaciers. J Glaciol 3 : 493–507
Otto-Bliesner BL (1996) Initiation of a continental ice sheet in a global climate model. J Geophys Res D12 : 16909–16920
Parrish JM, Parrish JT, Ziegler AM (1986) Permian-Triassic paleogeography and paleoclimatology and implications for Therapsid distribution. In: Hotton N II, McLean PD, Roth JJ, Roth EC (eds) The ecology and biology of mammal-like reptiles. Smithsonian Instruction Press, pp 109–131
Peltier WR (1994) Ice age paleotopography. Science 265 : 195–201
Peltier WR (1996) Mantle viscosity and Ice-age ice sheet topography. Science 273 : 1359–1364
Powell CM, Veevers JJ (1987) Namurian uplift in Australia and South America triggered the main Gondwanan glaciation. Nature 326 : 177–179
Rasbury ET, Hanson GN, Meyers WJ, Holt WE, Goldstein RH, Saller AH (1998) U-Pb dates of paleosols: constraints on late Paleozoic cycle durations and boundary ages. Geology 26 : 403–406
Raymo ME (1997) The timing of major climate terminations. Paleoceanography 12 : 577–585
Reeh N (1990) Parametrization of melt rate and surface temperature on the Greenland ice sheet. Polarforshung 59(3) : 113–128
Scotese CR (1986) Phanerozoic reconstructions: a new look at the assembly of Asia. Univ Texas Inst for Geophys Tech Rep 66
Scotese CR (1994) Late Carboniferous paleogeographic map. In: Klein GD (ed) Pangaea: paleoclimates, tectonics, and sedimentation during accretion, zenith, and breakup of a supercontinent. Geological Sociey of America Special Pap 288
Scotese CR, Golonka J (1982) Paleogeographic Atlas. Paleomap project, University of Texas-Arlington, Texas, USA
Shackleton NJ, Opdyke ND (1976) Oxygen isotope and paleomagnetic stratigraphy of Pacific core V28-239 late Pliocene to latest Pleistocene. Geol Soc Am Mem 145 : 449–464
Shackleton NJ et al. (1984) Oxygen isotope calibration of the onset of ice-rafting and history of glaciation in the north Atlantic region. Nature 307 : 620–623
Smith AG, Hallam A (1970) The fit of the southern continents. Nature 225 : 139–144
Tarasov L, Peltier WR (1997a) A high-resolution model of the 100 ky ice-age cycle. Ann Glaciol 25 : 58–65
Tarasov L, Peltier WR (1997b) Terminating the 100 ky ice age cycle. J Geophys Res D18 : 21665–21693
Tarasov L, Peltier WR (1999) The impact of thermo-mechanical ice-sheet coupling on a model of the 100 ky ice age cycle. J Geophys Res D8 : 9517–9545
Valdes PJ, Crowley TJ (1998) A climate model intercomparison for the Carboniferous. Paleoclimates 2 : 219–238
Visser JNJ (1997) A review of the Permo-Carboniferous glaciation in Africa. In: Martini IP (ed) Late glacial and postglacial environmental changes: Quaternary, Carboniferous–Permian, and Proterozoic. Oxford University Press, Oxford; pp 169–191
Wanless HR, Shepard FP (1936) Sea level and climatic changes related to late Paleozoic cycles. Geol Soc Am Bull 47 : 1177–1206
Wopfner H, Casshyap SM (1997) Transition from freezing to subtropical climates in the Permo–Carboniferous of Afro–Arabia and India. In: Martin PI (ed) Late glacial and postglacial environmental changes: Quaternary, Carboniferous–Permian, and Proterozoic. Oxford University Press
Zachos JC, Breza JR, Wise SW (1992) Early Oligocene ice sheet expansion on Antarctica: stable isotope and sedimentological evidence from the Kerguelen plateau, southern Indian ocean. Geology 20 : 569–573
Ziegler AM, Hulver ML, Rowley DB (1997) Permian world topography and climate. In: Martini PI (ed) Late glacial and postglacial environmental changes – Quaternary, Carboniferous–Permian and Proterozoic. Oxford University Press, Oxford, pp 111–146